Electrical and structural characterization of Si implanted homoepitaxially grown AlN

M. Hayden Breckenridge
Dept. of Material Science and Engineering
North Carolina State University
Raleigh, NC, USA
mhbrecke@ncsu.edu

Luis Hernandez-Balderrama
Dept. of Material Science and Engineering
North Carolina State University
Raleigh, NC, USA

Andrew Klump
Dept. of Material Science and Engineering
North Carolina State University
Raleigh, NC, USA
ajklump@ncsu.edu

Pramod Reddy
Adroit Materials
Cary, NC, USA
pramod@adroitmaterials.com

James Tweedie
Adroit Materials
Cary, NC, USA
james@adroitmaterials.com

Ronny Kirste
Adroit Materials
Cary, NC, USA
ronny@adroitmaterials.com

Ramón Collazo
Dept. of Material Science and Engineering
North Carolina State University
Raleigh, NC, USA
rcollaz@ncsu.edu

Zlatko Sitar
Dept. of Material Science and Engineering
North Carolina State University
Raleigh, NC, USA
sitar@ncsu.edu

***Abstract*— AlN is an attractive material for UV optoelectronics and high-power device applications; however, obtaining high n-type conductivity is still a challenge. Ion implantation may provide an avenue to realize electrical conductivities suitable for device operation. A novel annealing procedure to recover lattice damage is presented.**

Keywords—ion implantation, damage and recovery, annealing

I. INTRODUCTION

Aluminum nitride (AlN) is an attractive material for the development of next generation power electronic and high energy short wavelength (deep-UV) optoelectronic devices. AlN has a wide bandgap of 6.03 eV, Schottky barriers > 2eV and large breakdown field of 15 $MVcm^{-1}$ [1]–[5]. Controlling the doping and the compensation over several orders of magnitude are still technological challenges that need to be addressed to realize highly conducting regions in optoelectronics and low doped drift regions in power electronics. Typically, AlN is *n*-type doped by introducing Si donor atoms during epitaxial growth; however, the recorded free electron concentrations in epitaxially grown doped AlN is currently limited to concentrations $<10^{16}$ cm^{-3} at room temperature [6], [7].

The reduction in free carrier concentrations may be attributed to compensation due to the presence of high threading dislocation densities [8], [9], self-compensation likely by vacancy-Si complex formation [9], [10], and from the formation of a Si DX center that compensates the free electrons inside the material and results in high activation energies [6], [11], [12]. AlN films grown on foreign substrates (e.g. sapphire wafers) typically have high dislocation densities (DD) ($> 10^8$ cm^{-2}) despite various techniques to reduce DD [13]–[16]. In contrast, homoepitaxial AlN films grown on single crystal AlN substrates have DD < 10^4 cm^{-2} resulting in negligible DD based compensation [17]. Further, the lowering of the DD by growing on single crystal AlN substrates reduces self-compensation due to vacancy formation [9]. However, the self-compensation remains significant. Another form of compensation to consider is due to high concentrations of compensating carbon (C_N) observed in homoepitaxially grown AlN films. Additionally, the DX center formation associated with a large site relaxation of Si_{Al} and "pinning" of the bulk Fermi level resulting in a significantly higher binding energy than predicted by the hydrogenic model. Hence, a high Si activation energy (E_a ~ 250-320 meV) is typically observed in epitaxially doped AlN:Si which limits the overall free carrier concentration to < 10^{16} cm^{-3} [6], [12], [18].

However, Zeisel et al. showed that there should be an energy barrier between the shallow donor state, d0, and the deep donor DX- state [6]. Doping during growth limits the amount of bulk diffusion and surface kinetics dominate. Typically, energy barriers at the surface are significantly lower than at the bulk. Therefore, the concentration of Si atoms that relax to the DX- should be relatively high during growth, as observed experimentally. In the case of ion implantation, a non-equilibrium process, DX formation essentially occurs in the bulk and may be a more kinetically limited process. Hence, doping via ion implantation at low temperatures may significantly reduce the concentration of Si atoms that relax to the DX acceptor level state, ultimately allowing for higher free carriers to be realized.

Thus, compensating point defect control is the essential task required for attaining greater free electron concentrations in AlN films, making it possible to realize high-power and deep-UV optoelectronic devices. This may be achieved by either reducing the incorporation or generation of compensating defects and/or by suppressing the formation of a

978-1-5386-5349-4/18/$31.00 ©2018 IEEE

Si DX-center. Ion implantation is a well-known doping technique that provides the ability to control the lateral/vertical doping profile as well as the ability to implant with multiple doping species that are currently unavailable for MOCVD growth. In addition, ion implantation is not necessarily constrained by the growth conditions of the material that lower energetic barriers to the formation of compensating defects. However, little is known about the effects of ion implantation in AlN including the crystallographic damage and necessary recovery procedures. In this work we have studied how Si implantation parameters and activation annealing processes influence the structural and electrical properties of AlN films.

II. Experimental Setup

AlN substrates processed from AlN boules grown by physical vapor transport (PVT) were used in this study. More details of the AlN boule growth is described elsewhere [19]–[21]. AlN homoepitaxial films were grown via metal organic chemical vapor deposition (MOCVD) on single crystal AlN substrates. The AlN homoepitaxial films were grown at a temperature of 1100° C at a V/III ratio of 1000 and at a pressure of 20 Torr. Further details pertaining to AlN homoepitaxial growth are described elsewhere [22]. Using SRIM simulations and experimental data from literature [23], an acceleration voltage of 100 keV was chosen to achieve a Si peak concentration at approximately 100 nm. The target concentration was $1x10^{19}$ cm^{-3}, thus a Si dose of $1x10^{14}$ atoms/cm^2 was implanted into the homoepitaxial AlN film at room temperature at an angle of 7° (Fig. 1).

The implanted samples were characterized via secondary ion mass spectroscopy (SIMS) to determine the doping profile of the implanted Si atoms and confirm the background concentrations of oxygen and carbon. The crystal quality and lattice damage of each sample was assessed with the use of high-resolution x-ray diffraction (HR-XRD) following growth, ion implantation, and high temperature anneals. HR-XRD scans were recorded using a Philips X'Pert Materials Research Diffractometer system. The Cu Kα X-Rays were conditioned in point focus with a four-bounce Ge [220] monochromator. ω-rocking curve measurements were performed in open detector geometry. Post-implantation annealing conditions were 1200°C for 120 minutes with a nitrogen atmosphere and pressure of 100 Torr. Low Si concentration was observed near the surface via SIMS analysis, inhibiting any possibility of electrical contacts. Thus, approximately 80 nm of low Si concentration AlN was removed using an optimized BCl_3/Cl_2 recipe on a Trion Technology Minilock II reactive ion etcher (RIE). Two metal stacks were deposited onto the surface of the samples in a van der Pauw geometry using electron-beam evaporation. The first stack consisted of Ti/Al/Ni/Au and the second metal stack was V/Al/Ni/Au. Metal stacks were activated via a rapid thermal annealing process at 850°C for 60 s. I-V measurements were used to qualify the contacts. Then temperature dependent resistivity measurements were obtained using a four-point probe setup and a temperature range of 300-700 K.

III. Results and Discussion

Prior to implantation, ω-rocking curves were measured to evaluate the crystallinity of the AlN films grown via MOCVD

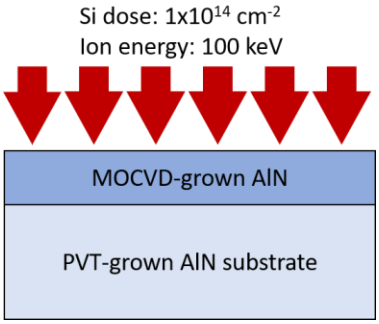

Fig. 1. Schematic of Si implantation into the surface of a MOCVD AlN film grown on PVT-grown AlN substrate. The implantation was perfomred at room temperature with a Si dose of $1x10^{14}$ cm^{-2} and ion energy of 100 keV.

[24]. The measured rocking curve full-width half maximum (FWHM) values of the (00.2) reflection of the grown AlN homoepitaxy were 12-18 arcsecs, near the resolution limit of the detector. These values indicate that crystal quality of the AlN substrate was inherited by the AlN film. The doping profile and background impurity concentrations were characterized via SIMS analysis. A gaussian profile was achieved with a Si peak concentration of $9x10^{18}$ cm^{-3} and a peak position of approximately 120 nm, as expected from SRIM/TRIM simulations. The oxygen and carbon concentrations were measured to be $5x10^{17}$ and $1x10^{17}$ cm^{-3}, respectively. XRD of the implanted sample showed a satellite peak at a lower 2θ angle than the primary AlN peak. The appearance of a satellite peak at lower angles is indicative of lattice distortion, implantation induced damage [25]. Upon annealing in the MOCVD reactor at 1200°C for 120 minutes, the satellite peak is no longer observed, indicating a reduction of lattice damage.

To improve the metal contacts, the topmost 80 nm of AlN was then removed using an optimized RIE BCl_3/Cl_2 recipe. A contact study was performed to determine a metal stack that would be suitable for the following electrical characterization. Two different metal contacts (V/Al/Ni/Au and Ti/Al/Ni/Au) were deposited onto the sample surface in the van der Pauw geometry. Both metal stacks were then activated using the same optimized RTA process. I-V measurements between two contact pads were used to compare the contacts (see Figure 2). The current that was achieved using the V-based stack was more than three orders of magnitude higher than the Ti-based stack. Temperature dependent resistivity measurements were then made to evaluate the electrical properties of the ion implanted AlN film. We estimate that the doping region is approximately 200 nm from the SIMS analysis, thus we used this value when calculating the conductivity. The temperature dependent conductivity is presented in Figure 3. We compare the Si implanted AlN sample (red triangles) to previous Si implanted AlN from literature (green squares) [23], and to epitaxially doped AlN (black triangles). At room temperature, the Si implanted AlN sample from this work has an order of magnitude higher conductivity than both the epitaxially doped sample and the implanted sample from literature. The Si activation energy (E_D) for each curve was determined by applying a linear fit and (1). The compensation in the ion implanted sample was assumed to be high due to some residual

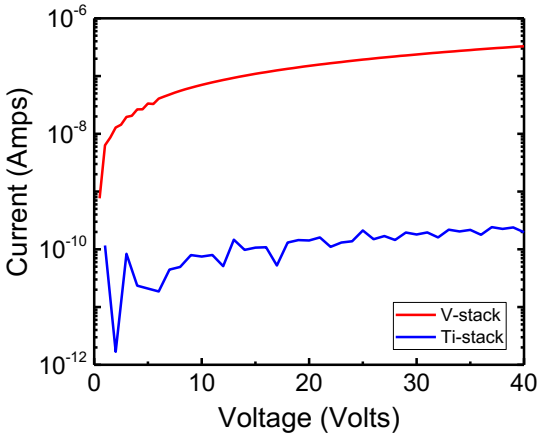

Fig. 2. I-V characteristics between two large contacts oriented in van der Pauw geometry Ti/Al/Ni/Au contacts (blue curve) and V/Al/Ni/Au contacts (red curve).

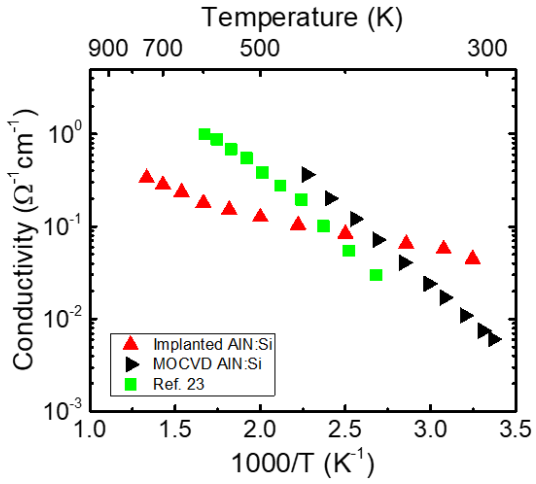

Fig. 3. Temperature dependent conductivities for the implanted sample after annealing at 1200°C for 120 minutes (red triangles), the epitaxially doped AlN:Si (black triangles), and a previous report of Si implanted AlN from literature [23] (green squares).

lattice damage being present and formation of vacancy complexes to form after annealing.

$$\sigma = \sigma_0 T^{-2} e^{\frac{E_D}{k_B T}} \quad (1)$$

The epitaxially doped sample and the ion implanted sample from literature were observed to have activation energies ~250 and ~290 meV, respectively. The ion implanted sample from this work had a significantly lower activation energy (~70 meV). This value is comparable to the expected value (75 meV) as predicted by the hydrogenic model for a Si atom in AlN. The higher conductivity and lower impurity ionization energy suggests that a majority of the Si atoms were at the shallow donor state compared to the relaxed DX state. We expect the compensation from residual damage and/or the formation of vacancy complexes are still a problem, thus motivating the need to further study the annealing process.

IV. Conclusion

In conclusion, we demonstrate the ability to use ion implantation to achieve a uniform doping profile in AlN with a peak depth of ~120 nm and a peak Si concentration of 9 x 10^{18} cm^{-3}. A novel annealing procedure was presented, allowing for significant lattice damage recovery. V-based metal stacks were observed to be superior *n*-type contacts compared to Ti-based contacts. Ultimately, we observe one order of magnitude increase in room temperature *n*-type conductivity compared to previous Si implantation in AlN and epitaxially doped AlN films. Low activation energy (~70 meV) was also observed for the Si implanted AlN sample, thus suggesting the formation of a DX-center was suppressed.

Acknowledgment

Partial financial support from NSF (DMR-1312582, ECCS-1508854, DMR-1508191, ECCS-1610992, ECCS-1653383), ARO (W911NF-15-2-0068, W911NF-16-C-0101), AFOSR (FA9550-17-1-0225) and DE-SC0011883 is greatly appreciated.

References

[1] H. Angerer *et al.*, "Determination of the Al mole fraction and the band gap bowing of epitaxial AlxGa1−xN films," *Appl. Phys. Lett.*, vol. 71, no. 11, pp. 1504–1506, Sep. 1997.

[2] Q. Guo and A. Yoshida, "Temperature Dependence of Band Gap Change in InN and AlN," *Jpn. J. Appl. Phys.*, vol. 33, no. 5R, p. 2453, May 1994.

[3] T. L. Chu and R. W. Kelm, "The Preparation and Properties of Aluminum Nitride Films," *J. Electrochem. Soc.*, vol. 122, no. 7, pp. 995–1000, Jul. 1975.

[4] T. Kinoshita *et al.*, "Fabrication of vertical Schottky barrier diodes on n-type freestanding AlN substrates grown by hydride vapor phase epitaxy," *Appl. Phys. Express*, vol. 8, no. 6, p. 61003, May 2015.

[5] P. Reddy *et al.*, "Schottky contact formation on polar and non-polar AlN," *J. Appl. Phys.*, vol. 116, no. 19, p. 194503, Nov. 2014.

[6] R. Zeisel *et al.*, "DX-behavior of Si in AlN," *Phys. Rev. B*, vol. 61, no. 24, pp. R16283–R16286, Jun. 2000.

[7] Y. Taniyasu, M. Kasu, and T. Makimoto, "Electrical conduction properties of n-type Si-doped AlN with high electron mobility (>100cm2V−1s−1)," *Appl. Phys. Lett.*, vol. 85, no. 20, pp. 4672–4674, Nov. 2004.

[8] E. C. H. Kyle, S. W. Kaun, P. G. Burke, F. Wu, Y.-R. Wu, and J. S. Speck, "High-electron-mobility GaN grown on free-standing GaN templates by ammonia-based molecular beam epitaxy," *J. Appl. Phys.*, vol. 115, no. 19, p. 193702, May 2014.

[9] I. Bryan *et al.*, "Doping and compensation in Al-rich AlGaN grown on single crystal AlN and sapphire by MOCVD," *Appl. Phys. Lett.*, vol. 112, no. 6, p. 62102, Feb. 2018.

[10] S. F. Chichibu *et al.*, "Impacts of Si-doping and resultant cation vacancy formation on the luminescence dynamics for the near-band-edge emission of Al0.6Ga0.4N films grown on AlN templates by metalorganic vapor phase epitaxy," *J. Appl. Phys.*, vol. 113, no. 21, p. 213506, Jun. 2013.

[11] Feneberg Martin *et al.*, "Sharp bound and free exciton lines from homoepitaxial AlN," *Phys. Status Solidi A*, vol. 208, no. 7, pp. 1520–1522, May 2011.

[12] R. Collazo *et al.*, "Progress on n-type doping of AlGaN alloys on AlN single crystal substrates for UV optoelectronic applications," *Phys. Status Solidi C*, vol. 8, no. 7–8, pp. 2031–2033, Jul. 2011.

[13] K. Nakano *et al.*, "Epitaxial lateral overgrowth of AlN layers on patterned sapphire substrates," *Phys. Status Solidi A*, vol. 203, no. 7, pp. 1632–1635, May 2006.

[14] H. Hirayama *et al.*, "222–282 nm AlGaN and InAlGaN-based deep-UV LEDs fabricated on high-quality AlN on sapphire," *Phys. Status Solidi A*, vol. 206, no. 6, pp. 1176–1182, Jun. 2009.

[15] J. Bai, M. Dudley, W. H. Sun, H. M. Wang, and M. A. Khan, "Reduction of threading dislocation densities in AlN/sapphire epilayers driven by growth mode modification," *Appl. Phys. Lett.*, vol. 88, no. 5, p. 51903, Jan. 2006.

[16] H. Miyake *et al.*, "Annealing of an AlN buffer layer in N2–CO for growth of a high-quality AlN film on sapphire," *Appl. Phys. Express*, vol. 9, no. 2, p. 25501, Jan. 2016.

[17] R. Dalmau *et al.*, "Growth and Characterization of AlN and AlGaN Epitaxial Films on AlN Single Crystal Substrates," *J. Electrochem. Soc.*, vol. 158, no. 5, pp. H530–H535, May 2011.

[18] B. Borisov *et al.*, "Si-doped AlxGa1−xN(0.56⩽×⩽1) layers grown by molecular beam epitaxy with ammonia," *Appl. Phys. Lett.*, vol. 87, no. 13, p. 132106, Sep. 2005.

[19] Z. G. Herro, D. Zhuang, R. Schlesser, R. Collazo, and Z. Sitar, "Seeded growth of AlN on N- and Al-polar 〈0001〉 AlN seeds by physical vapor transport," *J. Cryst. Growth*, vol. 286, no. 2, pp. 205–208, Jan. 2006.

[20] D. Zhuang, Z. G. Herro, R. Schlesser, and Z. Sitar, "Seeded growth of AlN single crystals by physical vapor transport," *J. Cryst. Growth*, vol. 287, no. 2, pp. 372–375, Jan. 2006.

[21] P. Lu *et al.*, "Seeded growth of AlN bulk crystals in m- and c-orientation," *J. Cryst. Growth*, vol. 312, no. 1, pp. 58–63, Dec. 2009.

[22] I. Bryan *et al.*, "Strain relaxation by pitting in AlN thin films deposited by metalorganic chemical vapor deposition," *Appl. Phys. Lett.*, vol. 102, no. 6, p. 61602, Feb. 2013.

[23] M. Kanechika and T. Kachi, "n-type AlN layer by Si ion implantation," *Appl. Phys. Lett.*, vol. 88, no. 20, p. 202106, May 2006.

[24] M. A. Moram and M. E. Vickers, "X-ray diffraction of III-nitrides," *Rep. Prog. Phys.*, vol. 72, no. 3, p. 36502, 2009.

[25] T. Niwa, T. Fujii, and T. Oka, "High carrier activation of Mg ion-implanted GaN by conventional rapid thermal annealing," *Appl. Phys. Express*, vol. 10, no. 9, p. 91002, Aug. 2017.